phosphate-buffered saline+ (PBS+)] described in (*9*). Nuclei were prepared from 4 to 20 × 10^7 HeLa by washing in PBS, resuspension in 10 ml of PB* diluted by 3 volumes of distilled water (PB*-diluted), incubation (2 min; 37°C), addition of 40 ml of PB*-diluted, incubation (15 min), Dounce homogenization (×10 to 15) to release 95 to 99% nuclei (assayed by phase-contrast microscopy), and adding 0.25% Triton X-100; after 5 min, nuclei were spun (250*g*; 5 min) through PB* with 10% glycerol, and the pellet was gently resuspended in PB*-BSA. Standard stereological procedures (*21*) showed that isolated nuclei were contaminated with <5% extranuclear ribosomes (detected by electron microscopy of Epon sections) (*18*) seen in whole cells. Greater than 95% of the nuclei excluded a 500-kD dextran conjugated with fluorescein isothiocyanate (FITC) (Sigma), so larger cytoplasmic ribosomes were unlikely to enter on isolation. Nuclei prepared as above, but without washing with Triton, incorporated the same amount of biotin (measured as in Fig. 2I); 94% also excluded a 70-kD dextran conjugated with FITC (Sigma) but not fluorescein-12-ATP.

9. A. Pombo *et al.*, *EMBO J.* **18**, 2241 (1999).
10. Calculations assume that a typical protein contains 5.8, 2, and 9.2% lysine, methionine, and leucine, respectively, and that ~2 × 10^6 ribosomes remain active on ~0.4 × 10^6 transcripts per cell (*23*). The following confirms that few peptides were completed in vitro. HeLa cells were labeled with [^{3}H]Leu in vivo (*12*) or in vitro (*11*), swollen (10 min; 4°C) in one-half dilution PB*-BSA, and broken (passage 20 times through 23 gauge needle), and nascent [^{3}H]peptides were separated from released (completed) ones by pelleting (20,000*g*; 45 min; 4°C). After in vivo labeling for 10 and 30 min, 22 and 48% ^{3}H were recovered in the supernatant, showing that many [^{3}H]peptides were released. Corresponding values after extension in vitro were only 4 and 8%, respectively. Even if all released peptides entered nuclei, they could not account for the nuclear signals seen.
11. Translation "mix" contained PB*-BSA, creatine phosphokinase (20 units/ml), 2.5 mM phosphocreatine, 0.25 mM GTP, tRNA (0.5 mg/ml) (Sigma; bovine liver), aminoacyl-tRNA synthetase (200 units/ml) (Sigma; bovine liver), protease inhibitors for mammalian cells (Sigma), and various supplements. $MgCl_2$ was also added in equimolar amounts to any NTPs. [Synthetases can be omitted when biotin-Lys-tRNA is used; then nucleoplasmic biotin incorporation (measured as in Fig. 2I) falls by 22%.] For Fig. 1, 2x concentrates of permeabilized cells (8 to 50 × 10^6/ml) or nuclei (4 to 20 × 10^7/ml) in suspension and the "mix" ± inhibitors were preincubated separately (3 min; 27.5°C), mixed, and incubated (27.5°C), and 100 μl was removed at various times and mixed with 350 μl of 2% SDS plus 50 μl of 5 M NaOH. After 30 min at 37°C, 100 μl of this were extracted with 10% trichloroacetic acid (TCA) and counted (*9*). For Fig. 1, A to C, supplements were 5 μM L-[4,5-^{3}H]Lys (86 Ci/mmol) + 50 μM amino acids minus Lys, 5 μM L-[4,5-^{3}H]Leu (147 Ci/mmol) + 50 μM amino acids minus Leu, and 1 μM biotin-lysine-tRNA from brewer's yeast (Boehringer) + 5 μM L-[4,5-^{3}H]Leu (147 Ci/mmol) + 50 μM amino acids minus Lys, respectively. For Fig. 1D, supplements were 200 μCi/ml of L-[^{35}S]Met (0.5 Ci/mmol) + 50 μM amino acids minus Met. After incubation, 250 μl was added to 10 ml of PB*, pelleted, rewashed in 10 ml of PB*, and resuspended in 150 μl of PB* diluted plus 1 mM $MgCl_2$, 1 mM dithiothreitol, human placental ribonuclease inhibitor (25 units/ml; Amersham), ribonuclease (RNase)–free deoxyribonuclease (100 units/ml), and protease inhibitors (as above); after 10 min at 37°C and addition of 100 μl of sample buffer, [^{35}S]proteins from 10^5 cells or 3 × 10^5 nuclei were run on 10 to 20% gradient acrylamide gels before autoradiography (*9*). For Figs. 2, 4A, and 5A, supplements were 1 μM biotin-lysine-tRNA from brewer's yeast (Boehringer) + 50 μM amino acids minus Lys; for Fig. 5B, 100 μM CTP and Br-UTP were also added. For Fig. 3, supplements were a 1/10 dilution BODIPY-Lys-tRNA (FluoroTect Green$_{Lys}$; Promega) + 50 μM amino acids minus Lys. For Fig. 4B, supplements were [^{3}H]Lys (100 μCi/ml; 86 Ci/mmol) + 50 μM amino acids minus Lys. After fixation in methanol, cells were washed in 5% TCA, rewashed in water, dried, and covered with dipping film (Ilford K.5) for 3 days; after developing, grain numbers were counted. Cycloheximide (1 mg/ml) was generally used to inhibit protein synthesis as it only reduced incorporation of [^{3}H]uridine by 25% (*12*).
12. See additional information at www.sciencemag.org/cgi/content/full/1061216/DC1.
13. M. Hollinshead, J. Sanderson, D. J. Vaux, *J. Histochem. Cytochem.* **45**, 1053 (1997).
14. Cells on cover slips were fixed (20 min; 4°C) in 4% paraformaldehyde in 250 mM Hepes (pH 7.4), antigens were indirectly immunolabeled with various antibodies (*12*, *24–26*), nucleic acids were counterstained with 20 μM TOTO-3 (Molecular Probes), images were collected with a confocal microscope (*9*), intensities over nucleoplasm and equivalent areas of the slide were measured (EasiVision software; Soft Imaging Systems), and data were exported to Excel (Microsoft) for background subtraction and analysis. Average intensities (confocal sections) of nucleoplasm and cytoplasm abutting the nucleus were determined and multiplied by the volume fraction of the two compartments (i.e., 400 and 673 μm^3) (*21*) to obtain relative contents. Incorporated BODIPY-Lys was directly detected after paraformaldehyde fixation.
15. U. F. Greber, L. Gerace, *J. Cell Biol.* **128**, 5 (1995).
16. F. J. Iborra, D. A Jackson, P. R. Cook, data not shown.
17. N. K. Chatterjee, H. W. Dickerman, T. A. Beach, *Arch. Biochem. Biophys.* **183**, 228 (1977).
18. For Fig. 5A, samples in suspension were fixed, treated with osmium, and embedded in Epon (*21*). For Fig. 5, B and C, they were fixed and embedded in LR White, indirectly immunolabeled with various antibodies (*12*, *27–29*) on ultrathin sections, and contrasted with uranyl acetate, and digital images were collected (*21*).
19. D. P. Eisinger, F. A. Dick, B. L. Trumpower, *Mol. Cell. Biol.* **17**, 5135 (1997).
20. O. L. Miller, B. A. Hamkalo, C. A. Thomas, *Science* **169**, 392 (1970).
21. F. J. Iborra, D. A. Jackson, P. R. Cook, *J. Cell Sci.* **111**, 2269 (1998).
22. P. R. Cook, *Science* **284**, 1790 (1999).
23. D. A. Jackson, A. Pombo, F. J. Iborra, *FASEB J.* **14**, 242 (2000).
24. M. K. Ray *et al.*, *Biochemistry* **32**, 5151 (1993).
25. J. R. Etchison, *J. Virol.* **61**, 2702 (1987).
26. F. Neumann, U. Krawinkel, *Exp. Cell Res.* **230**, 252 (1997).
27. W. V. Yotov, A. Moreau, R. St. Arnaud, *Mol. Cell Biol.* **18**, 1303 (1998).
28. F. J. Iborra *et al.*, *J. Histochem. Cytochem.* **40**, 1865 (1992).
29. M. B. Roth, A. M. Zahler, J. G. Gall, *J. Cell Biol.* **111**, 2217 (1990).
30. We thank the Wellcome Trust, Cancer Research Campaign [CRC], the Ministerio de Educacion y Cultura for support; N. Barclay, M. Clemens, U. Krawinkel, R. St.-Arnaud, and N. Sonenberg for kindly supplying plasmids and antibodies; and J. Bartlett and H. Kimura for their help.

30 March 2001; accepted 6 June 2001
Published online 21 June 2001;
10.1126/science.1061216
Include this information when citing this paper.

Snf1—a Histone Kinase That Works in Concert with the Histone Acetyltransferase Gcn5 to Regulate Transcription

Wan-Sheng Lo,[1] Laura Duggan,[1] N. C. Tolga Emre,[1] Rimma Belotserkovskya,[1] William S. Lane,[2] Ramin Shiekhattar,[1] Shelley L. Berger[1]*

Modification of histones is an important element in the regulation of gene expression. Previous work suggested a link between acetylation and phosphorylation, but questioned its mechanistic basis. We have purified a histone H3 serine-10 kinase complex from *Saccharomyces cerevisiae* and have identified its catalytic subunit as Snf1. The Snf1/AMPK family of kinases function in conserved signal transduction pathways. Our results show that Snf1 and the acetyltransferase Gcn5 function in an obligate sequence to enhance *INO1* transcription by modifying histone H3 serine-10 and lysine-14. Thus, phosphorylation and acetylation are targeted to the same histone by promoter-specific regulation by a kinase/acetyltransferase pair, supporting models of gene regulation wherein transcription is controlled by coordinated patterns of histone modification.

Posttranslational modifications of the NH_2-terminal tails within core histones are important determinants of transcriptional regulation. In recent years, specific covalent modifications on histone tails have been characterized, including acetylation, phosphorylation, ubiquitination, and methylation (*1*, *2*). Several transcriptional coactivators, such as the Gcn5 family, possess intrinsic histone acetyltransferase (HAT) activity (*3*), which correlates with gene activation (*4*, *5*). HATs are typically components of high molecular weight protein complexes that are recruited to specific promoters by interaction with DNA-bound transcriptional activators (*6*).

Histone phosphorylation is not as well understood as acetylation. Mitotic chromosome condensation is accompanied by histone H3

Ser-10 and Ser-28 phosphorylation, and recently several mitosis-specific Ser-10 kinases have been identified, including the Ipl1/Aurora family (*7*, *8*). Histone H3 Ser-10 phosphorylation is also correlated with mitogen-activated protein kinase signaling to the kinases Rsk2 and Msk1, and thereby to induction of immediate-early gene expression (*9*–*11*).

The existence of multiple covalent modifications in the histone tails suggests that some may function in similar pathways. In vitro, Ser-10 phosphorylation on histone H3 promotes Gcn5-mediated acetylation on nearby Lys-14 (*12*, *13*), and transcription of certain Gcn5-dependent genes in yeast requires Ser-10 (*12*). In addition, in epidermal growth factor–stimulated mammalian cells, histones possess dual modifications at Ser-10/Lys-14 or Lys-9/Ser-10 (*13*, *14*). Thus, phosphorylation and acetylation appear to be linked; however, this relation is not well understood, and the identification of functionally linked kinases and acetyltransferases should help to clarify these mechanisms.

The importance of histone H3 phosphorylation in transcriptional activation, and its mechanistic interconnection to acetylation by Gcn5, led us to investigate histone H3 kinases in *S. cerevisiae*. Whole-cell yeast extract was fractionated on Ni^{2+}-agarose, and the bound fraction was chromatographed over MonoQ ion-exchange resin. Four HAT complexes have previously been identified with this scheme and then purified (*15*–*18*) (Fig. 1A). We identified two histone H3 Ser-10 kinase activities (HK1 and HK2). For comparison, we examined Ser-28 kinase activity (*19*) and found one histone H3 Ser-28 kinase (HK3) (Fig. 1A) that was not overlapping with the Ser-10 activity. The fractionation profiles indicate that the kinases are not stable subunits of the acetylation complexes (Fig. 1A).

We chose the HK2 activity for further purification because it targeted Ser-10 and because it had stronger activity on Ser-10 than HK1. The purification scheme (seven chromatographic steps) is shown in Fig. 1B. We tracked the H3 Ser-10 kinase activity through purification using three assays: a radioactive in vitro kinase assay with intact histone H3, an immunoblot analysis with antibodies to Ser-10-Pi, and an in-gel kinase assay. The molecular size of the activity eluting from the Superose6 column was 300 to 400 kD (*20*). In-gel kinase assays of fractions containing the peak enzymatic activity from the MonoQ and Superose 6 columns (i.e., an early step and the last chromatographic step) indicated that the molecular size of the kinase itself is ~70 kD (Fig. 1C). One protein species that corresponded to the size of the active band was excised from the stained gel, digested with trypsin, and subjected to ion trap mass spectrometric sequencing, which identified the predominant protein in the sample as the kinase Snf1. Snf1 has a predicted molecular size of 72 kD, agreeing with the result of the in-gel assay analysis. No other predicted kinases in *S. cerevisiae* were present in the sample.

We determined whether Snf1 corresponds to the histone H3 Ser-10 kinase originally detected as HK2 activity from yeast. Snf1 was FLAG-epitope–tagged and purified with Ni^{2+}-agarose and MonoQ chromatography, followed by anti-FLAG immunoprecipitation (Fig. 2A). Five apparently stoichiometric protein bands were apparent, including a prominent ~70-kD band (Fig. 2B). This band corresponded to Snf1 as shown by anti-FLAG and anti-Snf1 immunoblots (Fig. 2C). The anti-Snf1 immunoblot detected the original MonoQ-purified material from the untagged strain as a slightly lower molecular weight species. Note that the FLAG is clipped off in a fraction of the Snf1-FLAG protein. All the bands that correspond to Snf1 in the anti-Snf1 immunoblot were also active in phosphorylating histone H3 in the in-gel kinase assay. Thus, Snf1 corresponds to the original HK2 activity (Fig. 1A) that was purified from yeast extract.

Bacterial glutathione-*S*-transferase (GST)–Snf1 phosphorylated free histone H3 at slightly higher levels than did GST-Ipl1 (Fig. 2D), which was previously shown to phosphorylate Ser-10 (*7*). GST-Ipl1 and GST-Snf1 had weak activity on nucleosomes, although previous experiments with bacterial histidine-tagged Ipl1 exhibited high nucleosomal activity (*7*). The histone H3 phosphorylation was specific in that it was the principal target within a mixture of histones. In addition, GST-Snf1 phosphorylated Ser-10 and not Ser-28 (*21*). Yeast-derived Snf1-FLAG also exhibited specificity for histone H3 (Fig. 2D). In addition, similar to Ipl1-FLAG, Snf1-FLAG phosphorylated histone H3 within nucleosomes, which are the presumed physiological substrate; the additional phosphorylated species in the original MonoQ fraction may correspond to H2B. The negative control, FLAG-tagged H4 acetyltransferase Esa1, had no histone kinase activity. Thus, the histone kinase specificity of recombinant Snf1 and native Snf1 are similar to the original HK2 activity, with the exception of a potential nucleosomal H2B activity of the original activity.

Snf1 regulates transcription of genes re-

[1]Molecular Genetics Program, The Wistar Institute, Philadelphia, PA 19104, USA. [2]Harvard Microchemistry and Proteomics Analysis Facility, Harvard University, Cambridge, MA 02138, USA.

*To whom correspondence should be addressed at The Wistar Institute, 3601 Spruce Street, Room 389, Philadelphia, PA 19104, USA. E-mail: berger@wistar.upenn.edu

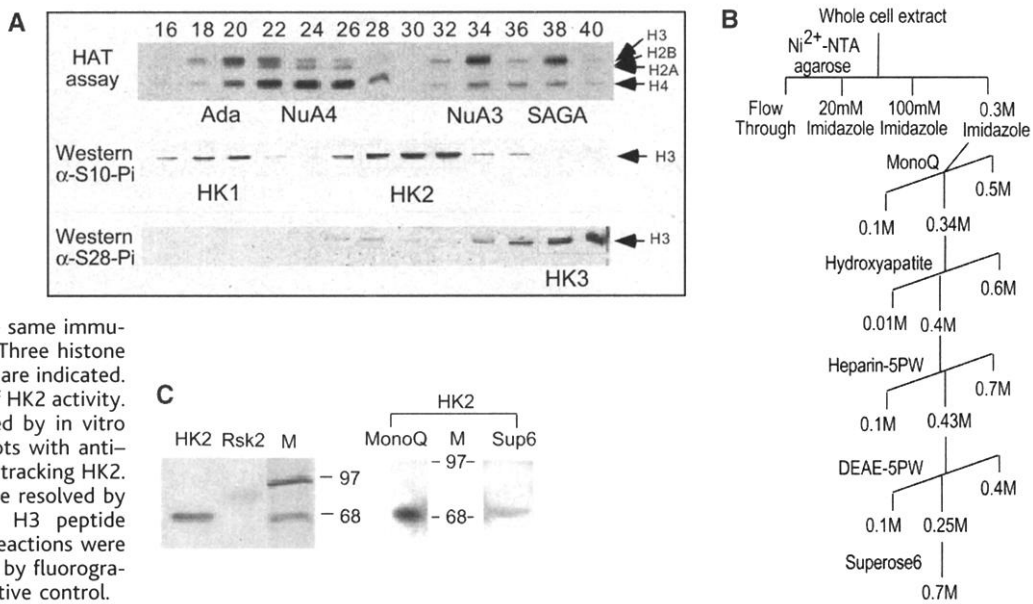

Fig. 1. (**A**) Purification of histone H3 Ser-10 and Ser-28 kinase activities from yeast, compared with H3 acetyltransferase activities. MonoQ column protein fractions were used in activity assays. (Upper panel) Fluorography of HAT assays on 15% SDS–polyacrylamide gel electrophoresis (SDS-PAGE) shows distinct HAT complexes (Ada, NuA4, NuA3, and SAGA). Arrows indicate core histones. (Middle panel) Immunoblots with anti–H3 Ser-10-Pi after kinase assays. (Lower panel) The same immunoblots, but with anti–H3 Ser-28-Pi. Three histone kinase activities (HK1, HK2, and HK3) are indicated. (**B**) Purification scheme for isolation of HK2 activity. H3 Ser-10 kinase activity was tracked by in vitro kinase assays followed by immunoblots with anti–H3 Ser-10-Pi. (**C**) In-gel kinase assays tracking HK2. MonoQ and Superose 6 fractions were resolved by 10% SDS-PAGE containing histone H3 peptide (amino acids 1 to 26). In-gel kinase reactions were performed, and bands were visualized by fluorography. Rsk2 (90 kD) was used as a positive control.

quired for growth in low-glucose media or alternate carbon sources such as sucrose (e.g., *SUC2*) (*22*, *23*), and of genes involved in the biosynthesis of inositol (e.g., *INO1*) (Fig. 3A) (*24*). Transcription of *INO1* also requires the acetyltransferase Gcn5 (*25*–*26*) (Fig. 3A). We examined whether histone modifications are directly required for transcription of *INO1*. The histone substitutions Ser-10→Ala (S10A), Lys-14→Ala (K14A), and S10A/K14A each reduced *INO1* transcription to a similar level (Fig. 3A). Thus, phosphorylation and acetylation of histone H3 appear to directly regulate transcription and therefore may be targets of Snf1 and Gcn5.

The level of histone H3 Ser-10 phosphorylation was compared to the level of *INO1* RNA at various times after shifting growth into media lacking inositol. In wild-type cells transcription increased to a maximum at 3 hours, and then decreased (Fig. 3B). In comparison, transcription in *snf1*$^-$ cells also increased, but was much lower at each time point. At the onset of inositol starvation, the level of Ser-10 phosphorylation was comparable in wild-type and *snf1*$^-$ cells, but was greatly diminished in *snf1*$^-$ cells when *INO1* transcription was nearing its maximum (Fig. 3B). These results demonstrate a correlation, in response to inositol starvation, between Snf1-dependent increase in *INO1* transcription and Snf1-dependent histone H3 phosphorylation.

These experiments suggested that phosphorylation of Ser-10 occurs in vivo during induction of the *INO1* gene, and that Snf1-dependent phosphorylation may lead to Gcn5-dependent acetylation. To test these models (Figs. 4A and 5A), we used chromatin immunoprecipitation (ChIP) to examine histone H3 covalent modifications directly at the endogenous *INO1* promoter. The first question is whether phosphorylation and acetylation occur on the same histone tails. Using a previously characterized dual-specificity antibody (*15*), we found that the level of dual Ser-10-Pi/Lys-14-Ac at the *INO1* promoter in the wild-type strain increased 14-fold upon gene induction in inositol-free media (Fig. 4A). Next, we examined

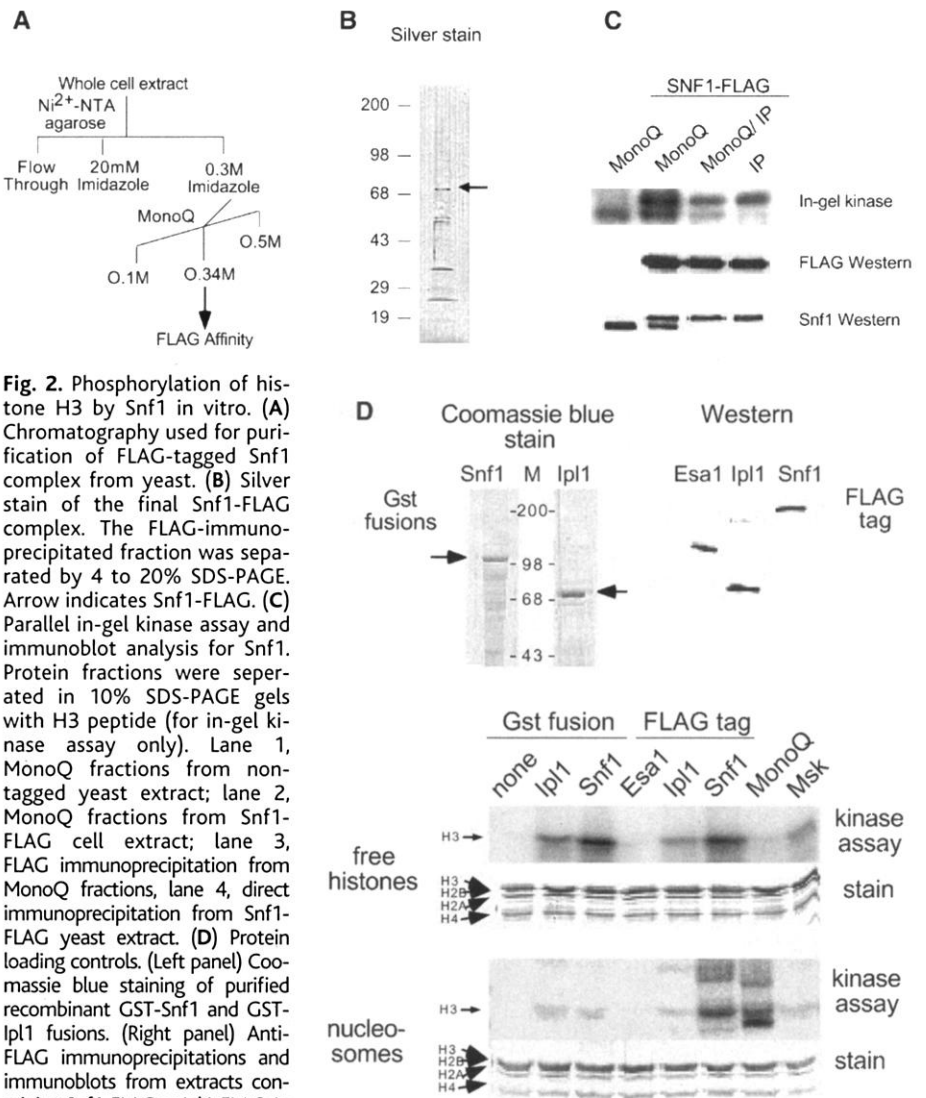

Fig. 2. Phosphorylation of histone H3 by Snf1 in vitro. (**A**) Chromatography used for purification of FLAG-tagged Snf1 complex from yeast. (**B**) Silver stain of the final Snf1-FLAG complex. The FLAG-immunoprecipitated fraction was separated by 4 to 20% SDS-PAGE. Arrow indicates Snf1-FLAG. (**C**) Parallel in-gel kinase assay and immunoblot analysis for Snf1. Protein fractions were seperated in 10% SDS-PAGE gels with H3 peptide (for in-gel kinase assay only). Lane 1, MonoQ fractions from non-tagged yeast extract; lane 2, MonoQ fractions from Snf1-FLAG cell extract; lane 3, FLAG immunoprecipitation from MonoQ fractions, lane 4, direct immunoprecipitation from Snf1-FLAG yeast extract. (**D**) Protein loading controls. (Left panel) Coomassie blue staining of purified recombinant GST-Snf1 and GST-Ipl1 fusions. (Right panel) Anti-FLAG immunoprecipitations and immunoblots from extracts containing Snf1-FLAG or Ipl1-FLAG. In vitro kinase assays were performed with free histones (5 μg, upper panel) or chicken mononucleosomes (20 μg, lower panel), with GST-Snf1 and GST-Ipl1 or Snf1-FLAG and Ipl1-FLAG. Reactions were separated in 15% SDS-PAGE gels and fluorographed. The corresponding gels were stained with Coomassie blue. GST alone and Esa1-FLAG were negative controls and Msk1 (Upstate Biotechnology) was a positive control.

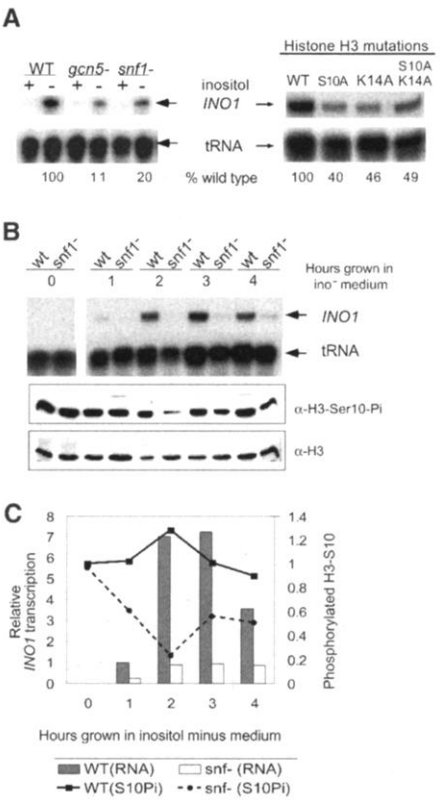

Fig. 3. (**A**) S1 nuclease analysis of *INO1* RNA. Yeast strains (wild type, *gcn5*$^-$, *snf1*$^-$, or histone H3 S10A, K14A, or S10A-K14A) were grown in high inositol/repressing conditions (+, minimal media with 100 μM inositol) or shifted to inositol starvation/inducing conditions (−, inositol-free minimal media) for 3 hours. RNA was purified for analysis. tRNA was used as the internal control. (**B**) Comparison of *INO1* RNA levels and histone H3 Ser-10 phosphorylation. Wild-type and *snf1*$^-$ strains were grown in repressing conditions, then shifted to media lacking inositol. At 0, 1, 2, 3, and 4 hours in inducing conditions, native histones and RNA were purified. (Upper panel) Transcriptional levels of *INO1* by S1 nuclease assay. Acid-purified proteins were separated on 15% SDS-PAGE and immunoblotted with anti–H3-Ser-10-Pi (middle panel) and anti-H3 (lower panel). (**C**) Histogram shows relative transcription level and histone phosphorylation. The relative *INO1* transcription levels in wild type (gray column) and *snf1*$^-$ (white column) during inositol starvation were shown after normalization to the wild-type level after 1-hour induction (left axis). The levels of histone H3 phosphorylation were shown after normalization to the wild-type level at time zero (right axis).

the effects of the substitutions S10A or K14A in histone H3, and of *gcn5*$^-$ or *snf1*$^-$ gene disruption. The *INO1* promoter was immunoprecipitated poorly from cells bearing substitution of either S10A, K14A, or S10A/K14A (Fig. 4B). In addition, immunoprecipitation of the *INO1* promoter was poor in cells bearing either a *snf1*$^-$ or *gcn5*$^-$ disruption (Fig. 4B). These results indicate that, at the *INO1* promoter, Snf1 modifies Ser-10 on histone H3, Gcn5 modifies Lys-14, and importantly, there is dual modification of Ser-10/Lys-14.

Our earlier observations indicated that Gcn5-mediated acetylation was promoted by Ser-10 phosphorylation in vitro (*12*). The identification of Snf1 as a Ser-10 kinase at the *INO1* promoter allowed us to directly test this proposed sequence, using monospecific antibodies for Ser-10 phosphorylation or Lys-14 acetylation, combined with strains disrupted for either Snf1 or Gcn5. The clear prediction is that Ser-10 phosphorylation will not require intact Lys-14 or Gcn5, but that Lys-14 acetylation requires both intact Ser-10 and Snf1 (Fig. 5A).

ChIP analysis of the *INO1* promoter indicated that, although Ser-10 phosphorylation was diminished by S10A substitution, it was not greatly affected by K14A substitution (Fig. 5B). Similarly, *snf1*$^-$ disruption diminished Ser-10 phosphorylation, but not *gcn5*$^-$ disruption, which instead increased Ser-10 phosphorylation. The results for Lys-14 acetylation were greatly contrasting. Both S10A and K14A substitution lowered Lys-14 acetylation (Fig. 5C), and both *snf1*$^-$ and *gcn5*$^-$ disruption lowered Lys-14 acetylation (Fig. 5D). These results demonstrate that (i) Ser-10 phosphorylation is required for acetylation at Lys-14 (but not vice versa) and (ii) Snf1 is the kinase responsible for initiating the pathway leading to acetylation of Lys-14.

In our earlier study we observed a reduction of *HO* transcription caused by S10A substitution (*12*). On the basis of the ChIP results described above, we predicted that histone acetylation at the *HO* promoter would be lowered by S10A substitution, but should not be affected by *snf1*$^-$ disruption. Indeed, the S10A substitution reduced acetylation at *HO*, similar to the effect on the *INO1* promoter, confirming that phosphorylation occurs at *HO* and is required for acetylation (Fig. 5D). However, in marked contrast to the *INO1* promoter, the *snf1*$^-$ mutation had little effect on acetylation at *HO* (Fig. 5D). This specificity indicates that, while Ser-10 phosphorylation indeed occurs at the *HO* promoter and is required for acetylation at Lys-14, the Snf1 kinase is not responsible for the phosphorylation. Thus, there is promoter specificity of Snf1 histone kinase activity, and presumably a different kinase carries out the histone phosphorylation at the *HO* promoter.

Our observations identify a histone kinase

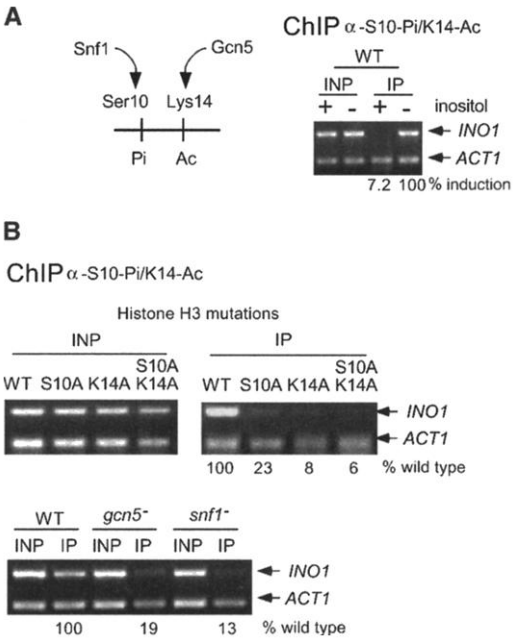

Fig. 4. Dual modification of histone H3 Ser-10 and Lys-14 at the *INO1* promoter. (**A**) (Left) Schematic model for the role of Snf1 and Gcn5 in H3 modifications at *INO1*. (Right) ChIP assay. Wild-type cells were grown in repressing or inducing conditions as indicated. Chromatin immunoprecipitation (ChIP) was done with H3 dual-modification (Ser-10-Pi/Lys-14-Ac) antibody (Upstate Biotechnology). The *INO1* [370 base pairs (bp)] and *ACT1* (275 bp) DNA sequences were identified by polymerase chain reaction and run on a 2% agarose gel. The relative immunoprecipitation efficiency was obtained by fluorography of ethidium bromide–stained gels (amount of immunoprecipitated DNA divided by input DNA) then normalization to the wild-type level in inositol starvation. The averages of immunoprecipitation efficiency from duplicate ChIP experiments are shown underneath each lane. The standard deviations were all <7%. (**B**) ChIP assay. Indicated strains (wild type and mutants) were grown in inducing conditions for 3 hours and immunoprecipitated with dual-modification antibody. The relative ChIP efficiencies were normalized to the wild-type level.

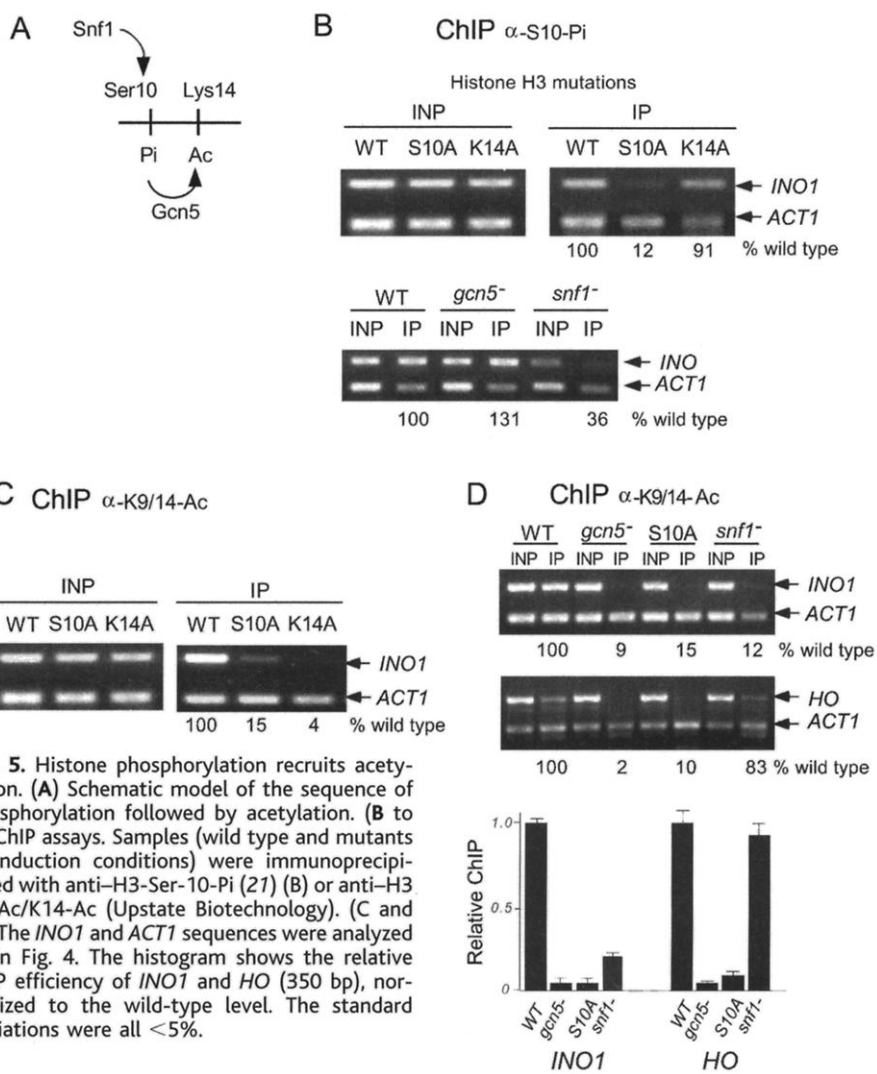

Fig. 5. Histone phosphorylation recruits acetylation. (**A**) Schematic model of the sequence of phosphorylation followed by acetylation. (**B** to **D**) ChIP assays. Samples (wild type and mutants in induction conditions) were immunoprecipitated with anti–H3-Ser-10-Pi (*21*) (B) or anti–H3 K9-Ac/K14-Ac (Upstate Biotechnology). (C and D). The *INO1* and *ACT1* sequences were analyzed as in Fig. 4. The histogram shows the relative ChIP efficiency of *INO1* and *HO* (350 bp), normalized to the wild-type level. The standard deviations were all <5%.

that is a previously known transcription-associated kinase, Snf1, and demonstrate that histone H3 Ser-10 phosphorylation by Snf1 leads to Gcn5-mediated acetylation at the *INO1* promoter. The linked and sequential modifications are required for full *INO1* transcriptional induction. The finding that Snf1 functions as a histone kinase suggests that other transcription-linked kinases may target histones for phosphorylation. The data support a targeting model where Snf1 is recruited to certain promoters, perhaps through the function of associated subunits. We have shown that Snf1 cofractionates in an apparent multisubunit complex, which may include the previously identified activating component Snf4 and substrate targeting subunits Sip2, Sip4, and Gal83 (*27*). These latter proteins may promote association of Snf1 with activators to direct catalysis to promoter-bound histones.

The experiments reported here demonstrate an interdependent pattern of histone modifications during gene activation. There is also evidence for multiple linked modifications (deacetylation leading to methylation) occurring during heterochromatic silencing in *Schizosaccharomyces pombe* and mammalian cells (*28*, *29*). The relation between histone modifications for silencing and those required for gene activation remains to be determined, although the balance between Lys-9 methylation and Ser-10 phosphorylation could represent a critical switch.

Why are there multiple modifications? Two general mechanisms are possible for the role of modifications. In the first, the electrostatic charge alterations may serve to directly alter nucleosome structure (*30*), and dual acetylation/phosphorylation would increase negative charge beyond either modification alone. In the second model, modifications provide an interaction surface for binding of proteins, an idea advanced as the "histone code" hypothesis (*2*, *31*). Phosphorylation of serine may provide an intermediate step, as discussed above, for binding of proteins in a sequence, or in tandem with acetylation, could provide a stronger or more selective binding surface. In either mechanism, multiple modifications could provide increased combinatorial and synergistic control during gene regulation.

References and Notes

1. E. M. Bradbury, *Bioessays* **14**, 9 (1992).
2. B. D. Strahl, C. D. Allis, *Nature* **403**, 41 (2000).
3. K. Struhl, Z. Moqtaderi, *Cell* **94**, 1 (1998).
4. L. Wang, L. Liu, S. L. Berger, *Genes Dev.* **12**, 640 (1998).
5. M.-H. Kuo, J. Zhou, P. Jambeck, M. E. A. Churchill, C. D. Allis, *Genes Dev.* **12**, 627 (1998).
6. C. E. Brown, T. Lechner, L. Howe, J. L. Workman, *Trends Biochem. Sci.* **25**, 15 (2000).
7. J.-Y. Hsu *et al.*, *Cell* **102**, 279 (2000).
8. R. Giet, D. M. Glover, *J. Cell Biol.* **152**, 669 (2001).
9. L. C. Mahadevan, A. C. Willis, M. J. Barratt, *Cell* **65**, 775 (1991).
10. P. Sassone-Corsi *et al.*, *Science* **285**, 886 (1999).
11. S. Thomson *et al.*, *EMBO J.* **18**, 4779 (1999).
12. W. S. Lo *et al.*, *Mol. Cell* **5**, 917 (2000).
13. P. Cheung *et al.*, *Mol. Cell* **5**, 905 (2000).
14. A. L. Clayton, S. Rose, M. J. Barratt, L. C. Mahadevan, *EMBO J.* **19**, 3714 (2000).
15. P. A. Grant *et al.*, *Genes Dev.* **11**, 1640 (1997).
16. S. Allard *et al.*, *EMBO J.* **18**, 5108 (1999).
17. A. Eberharter *et al.*, *Mol. Cell. Biol.* **19**, 6621 (1999).
18. S. John *et al.*, *Genes Dev.* **14**, 1196 (2000).
19. H. Goto *et al.*, *J. Biol. Chem.* **274**, 25543 (1999).
20. W.-S. Lo *et al.*, data not shown.
21. Supplementary Web material is available on *Science* Online at www.sciencemag.org/cgi/content/full/293/5532/1142/DC1.
22. A. Woods *et al.*, *J. Biol. Chem.* **269**, 19509 (1994).
23. M. Carlson, *Curr. Opin. Microbiol.* **2**, 202 (1999).
24. M. K. Shirra, K. M. Arndt, *Genetics* **152**, 73 (1999).
25. S. M. Roberts, F. Winston, *Genetics* **147**, 451 (1997).
26. K. J. Pollard, C. L. Peterson, *Mol. Cell. Biol.* **17**, 6212 (1997).
27. D. G. Hardie, D. Carling, M. Carlson, *Annu. Rev. Biochem.* **67**, 821 (1998).
28. S. Rea *et al.*, *Nature* **406**, 593 (2000).
29. S. L. Berger, *Science* **292**, 64 (2001)
30. J. J. Hayes, J. C. Hansen, *Curr. Opin. Genet. Dev.* **11**, 124 (2001).
31. B. M. Turner, *Bioessays* **22**, 836 (2000).

32. We thank F. Winston, M. Grunstein, C. D. Allis, H. Goto, and M. Inagaki for plasmids, strains, and antibodies, and N. Keiser for assistance with construction of the K14A yeast strain. We thank P. Lieberman, G. Moore, D. Sterner, K. Wang, and members of the Berger laboratory for discussions. Supported by National Institute of General Medical Sciences (S.L.B. and R.S.) and NSF (S.L.B.).

7 May 2001; accepted 11 July 2001

Argonaute2, a Link Between Genetic and Biochemical Analyses of RNAi

Scott M. Hammond,[1,2] Sabrina Boettcher,[1] Amy A. Caudy,[3] Ryuji Kobayashi,[1] Gregory J. Hannon[1,3]*

Double-stranded RNA induces potent and specific gene silencing through a process referred to as RNA interference (RNAi) or posttranscriptional gene silencing (PTGS). RNAi is mediated by RNA-induced silencing complex (RISC), a sequence-specific, multicomponent nuclease that destroys messenger RNAs homologous to the silencing trigger. RISC is known to contain short RNAs (~22 nucleotides) derived from the double-stranded RNA trigger, but the protein components of this activity are unknown. Here, we report the biochemical purification of the RNAi effector nuclease from cultured *Drosophila* cells. The active fraction contains a ribonucleoprotein complex of ~500 kilodaltons. Protein microsequencing reveals that one constituent of this complex is a member of the Argonaute family of proteins, which are essential for gene silencing in *Caenorhabditis elegans*, *Neurospora*, and *Arabidopsis*. This observation begins the process of forging links between genetic analysis of RNAi from diverse organisms and the biochemical model of RNAi that is emerging from *Drosophila* in vitro systems.

RNA interference is a process whereby double-stranded RNA (dsRNA) induces the silencing of cognate genes (*1*). Posttranscriptional silencing phenomena have also been observed in plants (e.g., PTGS) and fungi (e.g., quelling), and genetic studies indicate that these are likely to be mechanistically related to RNAi. Moreover, RNAi per se has been demonstrated in a variety of experimental systems, including insects, protozoans, and mammals (*2*).

A synthesis of in vivo and in vitro experiments has led to a mechanistic model for RNAi/PTGS. Silencing is initiated by exposure of a cell to dsRNA. This "trigger" may be introduced experimentally or may derive from endogenous sources such as viruses, transgenes, or cellular genes (e.g., transposons). Double-stranded RNAs are processed into discrete ~21- to 25-nucleotide (nt) RNA fragments known as siRNAs (small interfering RNAs) (*3*, *4*). These small RNAs join a multicomponent nuclease complex, RISC, and guide that enzyme to its substrates through conventional base-pairing interactions (*5*). Recognition of mRNAs by RISC leads to their destruction.

To date, mechanistic studies have approached RNAi/PTGS from two standpoints. Genetic studies have identified nearly a dozen genes that affect the dsRNA response. These include genes that encode putative nucleases [*mut-7* (*6*), helicases [*qde-3* (*7*), *SDE3* (*8*), *mut-6* (*9*)], RNA-dependent RNA polymerases [e.g., *ego-1* (*10*), *qde-1* (*11*), *SDE1* (*12*)/*SGS2* (*13*)], and members of the Argonaute family [*rde-1* (*14*), *qde-2* (*15*),

[1]Cold Spring Harbor Laboratory, Cold Spring Harbor, NY 11724, USA. [2]Genetica Inc., 1 Kendall Square, Building 600, Cambridge, MA 02138, USA. [3]Watson School of Biological Sciences, Cold Spring Harbor Laboratory, 1 Bungtown Road, Cold Spring Harbor, NY 11724, USA.

*To whom correspondence should be addressed. E-mail: hannon@cshl.org